Journal of Medicinal Chemistry Article

J. Med. Chem. **2010,** *53,* 3919–3926 **3919**
DOI: 10.1021/jm901489k

Peptide Nucleic Acids Conjugated to Short Basic Peptides Show Improved Pharmacokinetics and Antisense Activity in Adipose Tissue

Edward V. Wancewicz,[†] Martin A. Maier,[§] Andrew M. Siwkowski,[†] Klaus Albertshofer,[∥] Theodore M. Winger,[⊥] Andres Berdeja,[†] Hans Gaus,[†] Timothy A. Vickers,[†] C. Frank Bennett,[†] Brett P. Monia,[†] Richard H. Griffey,[#] Christopher J. Nulf,[‡] Jiaxin Hu,[‡] David R. Corey,[‡] Eric E. Swayze,[†] and Garth A. Kinberger*[,†]

[†]*Isis Pharmaceuticals, Inc., 1896 Rutherford Road, Carlsbad, California 92008, and* [‡]*Departments of Pharmacology and Biochemistry, University of Texas Southwestern Medical Center, Dallas, Texas 75390.* [§]*Current Address: Alnylam Pharmaceuticals, 300 Third Street, Cambridge, Massachusetts 02142.* [∥]*Current Address: Departments of Chemistry and Molecular Biology The Scripps Research Institute, 10550 North Torrey Pines Road, La Jolla, California 92037.* [⊥]*Current Address: Advanced Liquid Logic, Inc., PO Box 14025, Research Triangle Park, North Carolina 27709.* [#]*Current Address: SAIC, 10260 Campus Point Drive, San Diego, California 92121*

Received October 7, 2009

A peptide nucleic acid (PNA) targeting a splice junction of the murine PTEN primary transcript was covalently conjugated to various basic peptides. When systemically administered to healthy mice, the conjugates displayed sequence-specific alteration of PTEN mRNA splicing as well as inhibition of full length PTEN protein expression. Correlating activity with drug concentration in various tissues indicated strong tissue-dependence, with highest levels of activity observed in adipose tissue. While the presence of a peptide carrier was found to be crucial for efficient delivery to tissue, little difference was observed between the various peptides evaluated. A second PNA-conjugate targeting the murine insulin receptor primary transcript showed a similar activity profile, suggesting that short basic peptides can generally be used to effectively deliver peptide nucleic acids to adipose tissue.

Introduction

Peptide nucleic acids (PNAs[a]) are nucleic acid analogues in which the natural sugar−phosphate backbone is replaced by an achiral, uncharged pseudopeptide backbone composed of (2-aminoethyl)glycine units as shown in Figure 1.[1] Complementary DNA or RNA sequences are recognized through standard Watson−Crick base pairing, while the neutral PNA backbone eliminates interstrand charge repulsion during hybridization thereby enhancing thermal stability.[2] Because of their unnatural backbone, PNAs are poor substrates for proteases or nucleases, which makes them extraordinarily stable against enzymatic degradation.[3] However, the application of unmodified PNAs as antisense therapeutics thus far has been limited by their low solubility under physiological conditions, insufficient cellular uptake, and poor biodistribution due to rapid plasma clearance and excretion.[4,5]

A synthetically feasible approach to improve the physicochemical and biological properties of PNA lies in conjugation to short synthetic peptide carriers. We recently evaluated various simple basic peptides designed to serve as solubility enhancers as well as delivery vehicles. In two separate peptide SAR series, the structural requirements for efficient cellular uptake and potent

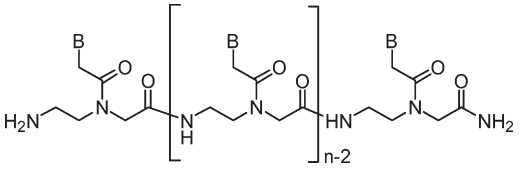

Figure 1. Generic depiction of a peptide nucleic acid (PNA) where B represents the nucleobases and *n* is equal to the number of subunits that comprise the PNA structure.

inhibitory activity of the corresponding PNA conjugates have been elucidated in cell culture.[6,7] Pharmacokinetic studies indicated that the conjugates rapidly distributed to a variety of tissues while their rates of elimination via excretion were dramatically reduced compared to unmodified PNA.

Peptide nucleic acids do not support ribonuclease H (RNase H) mediated cleavage of RNA,[8] which has been shown to be the predominant mechanism of action for DNA-like antisense oligonucleotides.[9] Therefore, an antisense strategy involving PNA-based inhibitors must rely on mechanisms such as alteration of pre-mRNA splicing, translational arrest or inhibition of transcription. Previously, we identified a peptide nucleic acid, which redirects splicing of murine CD40 mRNA thereby inhibiting CD40 expression.[10] While CD40 represents a therapeutically interesting target, its expression is limited to B-lymphocyte, dendritic, and endothelial cells and macrophage subpopulations of a few tissues like spleen and lymph nodes. We reasoned that a more broadly expressed target protein would be advantageous for investigating the in vivo pharmacology of PNA−peptide conjugates and to determine whether such constructs could offer any

*To whom correspondence should be addressed. Phone: 760-603-2685. E-mail: gkinberger@isisph.com.

[a]Abbreviations: BUN, blood urea nitrogen; BCL_1, B-cell lymphoma; FITC, fluorescein isothiocyanate; hR, homoarginine; IR, insulin receptor; ip, intraperitoneal; MOE, 2′-*O*-methoxyethyl; PNA, peptide nucleic acid; PTEN, phosphatase and tensin homologue; PTO, phosphorothioate oligonucleotides; RNase H, ribonuclease H; RT-PCR, rverse transcription polymerase chain reaction; T_K, (2-aminoethyl)lysine T; UTC, untreated control.

Published on Web 04/26/2010

advantage over other chemistries such as 2′-*O*-methoxyethyl (MOE) gapmers, which support RNase H-mediated cleavage of the mRNA target. We chose murine phosphatase and tensin homologue (PTEN) as a model target because it is expressed in a wide variety of tissues, allowing PK/PD relationships of PNA to be examined via PTEN protein reduction. Insulin receptor was also chosen as a model target for its therapeutic relevance.

Herein, we report the results of in vivo studies where PNA−peptide conjugates were analyzed along with appropriate controls. PNA−peptide conjugates were designed to target murine PTEN or insulin receptor, and liver, kidney, as well as adipose tissues were examined for PNA dependent alteration of mRNA splicing. On the basis of the in vivo results, a tissue dependent PK/PD relationship for PNA is discussed. Our data suggest that basic peptides conjugated to PNA can be used to effectively deliver peptide nucleic acids to, and elicit pharmacology in adipose tissue.

Results and Discussion

Identification of a Potent PNA Inhibitor of PTEN Expression. PTEN was chosen as the target for this study because it is ubiquitously expressed in a wide variety of tissues. The PTEN protein is present in different isoforms. The translation of the full length mRNA transcript results in the full length protein and is the most abundant isoform. A smaller and less abundant isoform is expressed through alternative splicing where exon 4 is omitted (−exon 4) from the primary transcript. This deletion results in a frame shift in the downstream codons of exons 5−9 (Scheme 1). In previous screens, two uniform 2′-*O*-MOE 20-mer oligonucleotides (**1** and **2**) targeting two different splice sites were found to effectively alter splicing of the primary murine PTEN transcript and inhibit expression of full length protein. On the basis of their sequence, two sets of PNA pentadecamers were designed and screened in a murine B-cell lymphoma (BCL_1) cell line for their potential to alter splicing and reduce the expression of PTEN protein (Table 1).

Peptide nucleic acid **3** was the most potent PNA of this set. PNA **3** demonstrated alteration of splicing of PTEN RNA where the full length transcript was reduced and the alternatively spliced product was enhanced as determined by quantitative reverse transcription polymerase chain reaction (RT-PCR) analysis (data not shown). The alternatively spliced transcript was cloned and sequenced, confirming the omission of exon 4, resulting in a frame shift in the downstream codons of exons 5−9. Figure 2 shows the effect of PNA **3** on PTEN protein expression as determined by Western blot analysis. Clearly, full length PTEN protein is reduced in a dose dependent manner. However, the protein associated with the alternatively spliced transcript is not observed because the C-terminal portion of the protein recognized by the antibody is lost in the alternatively spliced product.

Scheme 1. Redirection of Splicing by Antisense Oligonucleotide (—) from the Full Length PTEN mRNA Transcript to the Alternatively Spliced Product Where Exon 4 Is Omitted

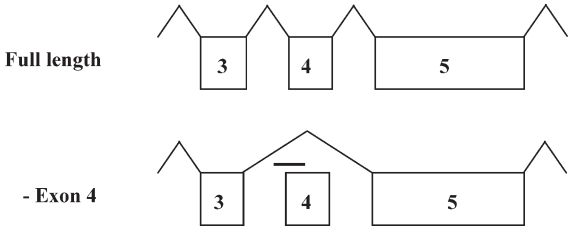

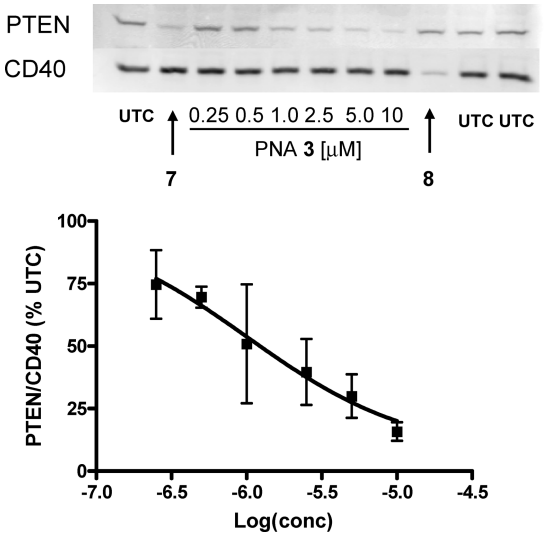

Figure 2. Dose-dependent inhibition of PTEN protein expression by PNA **3**. BCL_1 cells were electroporated with either no compound, untreated control (UTC), or compound at the given concentrations. Cells were harvested 62 h post electroporation. PTEN and CD40 protein expression were measured by Western blot. An antiPTEN phosphorothioate oligonucleotide with 2′-*O*-MOE wings and a 2′-deoxyribonucleotide gap (gapmer control **7**) and a PNA 15-mer targeting CD40 (**8**) were used as positive and negative controls, respectively. PTEN protein was normalized to CD40 protein and plotted. The values shown in the graph represent the averages (n = 3 per group) and their corresponding standard deviations.

Table 1. Sequence, Position, and IC_{50} Values of the Parent 2′-*O*-MOE 20-Mers, the PNA Oligomers As Well As the 2′-*O*-MOE Gapmer and the AntiCD40 PNA as Positive and Negative Controls, Respectively

compd	sequence N to C-terminus (5′ to 3′)	position on PTEN transcript	IC_{50} [μM][a]
1	CTCAGCACATCTACAAGAAA[b]	intron 3:exon 4	1.0
2	ATAGTTTCACCTAGAGAAAG	intron 8: exon 9	2.2
3	CTCAGCACATCTACA-Lys	intron 3:exon 4	1.0
4	ATAGTTTCACCTAGA-Lys	intron 8: exon 9	3.2
5	TTCACCTAGAGAAAG-Lys	intron 8: exon 9	3.0
6	AGTTTCACCTAGAGA-Lys	intron 8: exon 9	2.4
7	CTGCTAGCCTCTGGATTTGA[c]	exon 9	3.2
8	CACAGATGACATTAG-Lys	antiCD40	0.9[d]

[a] IC_{50} values were determined by Western blot analysis of PTEN protein expression. [b] Uniform 2′-*O*-MOE (underlined) phosphorothioate. [c] phosphorothioate oligonucleotides (PTO) with 2′-*O*-MOE (underlined) and a 2′-deoxyribonucleotide gap. Cells were electroporated to facilitate the uptake of the oligomers. [d] CD40 cell surface protein expression was determined by flow cytometry using a fluorescein isothiocyanate (FITC) labeled antiCD40 antibody.[10]

In Vivo Evaluation of the Octa(L-lysine) Conjugate 9 and Its Controls. On the basis of our earlier studies with Kole and coworkers,[11,12] we previously investigated the use of simple basic peptides, such as octa(L-lysine) and analogues as well as basic amphipathic model peptides, for cellular delivery of an antisense PNA targeting murine CD40.[6,7] The SAR studies revealed some of the structural requirements for effective cellular delivery and a few representative examples were evaluated for their biodistribution in healthy mice. They were rapidly cleared from circulation and distributed to a variety of tissues, namely liver, kidney, spleen, and mesenteric lymph nodes and showed only modest elimination via excretion within the time frame of the studies. While the results demonstrated that short basic peptides can be utilized to improve upon the intrinsically poor uptake and PK properties of PNA, the question remained whether these PK improvements would translate into potent antisense effects in the tissues to which the PNA conjugates were delivered.

To address this question, we synthesized the octa(L-lysine) conjugate **9** (Figure 3), a minimally modified PNA conjugate **10** with a net positive charge just high enough to provide sufficient solubility under physiological conditions, and an octa(L-lysine)-bearing PNA **11** with four mismatches to the complementary target sequence. To reduce the number of extra lysines required to render the minimally modified compound **10** soluble under physiological conditions, the PNA sequence was extended by one unit using a PNA T monomer with a (2-aminoethyl)lysine backbone (T_K) bearing a positively charged lysine side chain. The extended sequence is still fully complementary to its target site on the PTEN transcript. The gapmer **7** and the uniformly 2′-*O*-MOE-modified oligonucleotide **1**, both with full phosphorothioate backbone, were used as positive controls (Table 2).

The compounds were administered intraperitoneally (ip) three times a week for two weeks to healthy male Balb/c mice (n = 4 per group), and the animals were sacrificed 48 h after the last dose. None of the groups showed any significant body weight change or changes in serum chemistry such as AST, ALT, blood urea nitrogen (BUN), bilirubin, glucose, and triglycerides compared to the saline-treated control group. Groups receiving the 40 mg/kg dose of the octa(L-lysine) conjugates **9** or **11** had elevated spleen weights up to 145% as compared to that of the saline treated control group. Western blot analysis of liver samples showed that none of the PNA conjugates effectively altered splicing enough to reduce PTEN protein expression. Only the positive control **7** showed significant inhibition of PTEN protein expression (Figure S2, Supporting Information).

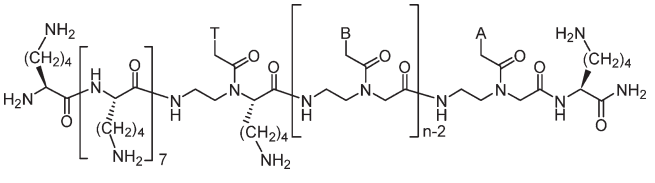

Figure 3. Octa(L-lysine) PNA conjugate **9**, which has a PNA T monomer with a (2-aminoethyl)lysine backbone modification (T_K) between the PNA and peptide portion of the conjugate.

Quantitative RT-PCR analysis of liver samples essentially corroborated the Western blot result in that none of the PNA conjugates showed a characteristic alteration of PTEN splicing. The phosphorothioate gapmer **7** caused downregulation of total PTEN message (both isoforms) as expected for an antisense oligonucleotide that operates through activation of RNase H. The uniform 2′-*O*-MOE control **1**, which targets the same splice junction as the PNAs, showed modest downregulation of full length transcript with upregulation of the alternatively spliced product (Figure S3a, Supporting Information). In kidney, **9** elicited moderate activity at the high dose with the full length transcript being reduced to about 70% and the isoform lacking exon 4 being upregulated to about 185% of the of the saline-treated control (Figure S3b, Supporting Information). All of the other groups including the one treated with the gapmer showed no evidence of activity.

In contrast to liver and kidney, in white adipose tissue, the octa(L-lysine) conjugate **9** showed a dose-dependent downregulation of full length PTEN transcript with concomitant upregulation of its alternatively spliced isoform (Figure 4a). At a dose of 40 mg/kg, the level of activity was comparable to that observed for the gapmer control **7**, administered at a lower dose of 25 mg/kg. The activity of the uniform 2′-*O*-MOE oligonucleotide **10** in adipose tissue was found to be marginal with the alternatively spliced isoform being upregulated but the full length transcript being unaltered. The mismatch control **11** was inactive at both doses, which confirmed the sequence-specificity of the observed effect. The minimally modified PNA **10** was inactive at both doses, demonstrating that the presence of the full length peptide vector was crucial for activity in this tissue. Western blot analysis confirmed the mRNA results in that only the gapmer **7**, and the high dose of the antisense PNA conjugate **9** showed significant and comparable downregulation of PTEN protein (Figure 4b).

Tissue concentrations from the 40 mg/kg dose of the octa(L-lysine) conjugate **9** and the minimally modified PNA **10** were determined by analyzing liver, kidney, and adipose tissue samples with an ELISA-based assay where an oligonucleotide with a sequence complementary to the PNA bearing digoxigenin at the 5′-end and biotin at the 3′-end was utilized as the probe (Table 3). Therefore, the tissue concentration results obtained for these measurements reflect the PNA concentration which includes intact drug as well as any potential metabolites. The results shown in Table 3 illustrate that the full length peptide carrier, octa(L-lysine), substantially enhanced drug accumulation in liver and adipose tissue approximately 5-fold and 20-fold, respectively, in comparison to the di(L-lysine) peptide carrier. However, in kidney, the difference in molar concentrations of PNA **9** and **10** were smaller.

Table 2. Sequence and Chemistry of the Octa(L-lysine) Conjugate **9** and Its Controls

compd	sequence N to C-terminus (5′ to 3′)	dosing	chemistry
9	$(Lys)_8$-T_K[a]CTCAGCACATCTACA-Lys	10 or 40 mg/kg, 3×/wk, 2 wks	PNA-peptide
10	$(Lys)_2$-T_KCTCAGCACATCTACA-Lys	10 or 40 mg/kg, 3×/wk, 2 wks	minimally modified PNA
11	$(Lys)_8$-T_KCT*A*[b]*AC*CACATCT*CG*A-Lys	10 or 40 mg/kg, 3×/wk, 2 wks	PNA-peptide mismatch
1	CTCAGCACATCTACAAGAAA	40 mg/kg, 3×/wk, 2 wks	uniform 2′-*O*-MOE PTO
7	CTGCTAGCCTCTGGATTTGA	25 mg/kg, 3×/wk, 2 wks	2′-*O*-MOE gapmer PTO

[a] T_K, (2-aminoethyl)lysine T. [b] Mismatched bases to the parent sequence appear in italics.

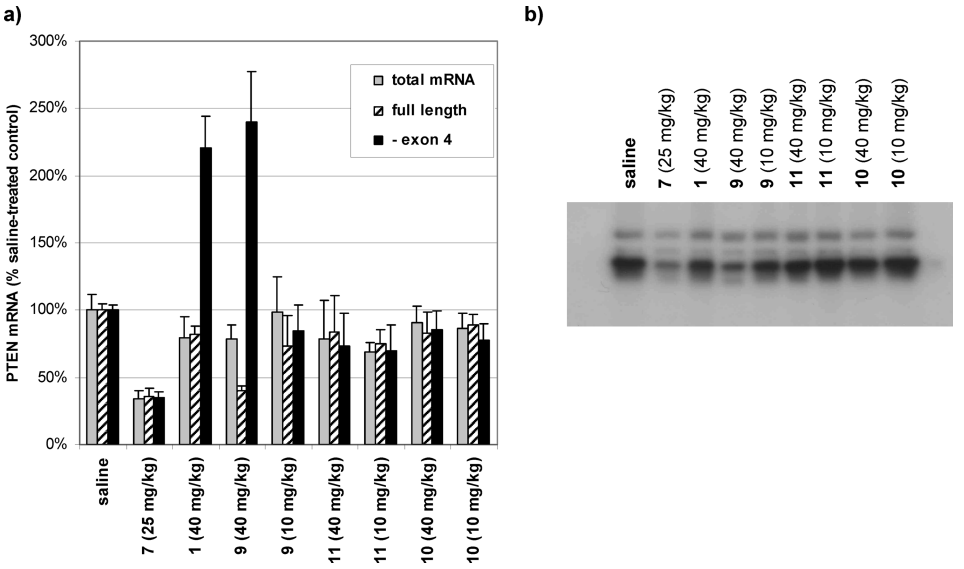

Figure 4. Antisense effects in adipose tissue: (a) quantitative RT-PCR analysis of PTEN mRNA, (b) Western blot analysis of PTEN protein (multiple bands are due to antibody artifact).

Table 3. Tissue Concentrations of the Octa(L-lysine) Conjugate **9** and the Minimally Modified PNA **10**[a]

tissue	compd	concentration [μg/g]	concentration [μM]
liver	**9**	591 ± 51	108 ± 9
	10	133 ± 45	28 ± 10
kidney	**9**	2239 ± 16	408 ± 3
	10	1673 ± 29	355 ± 6
adipose tissue	**9**	432 ± 282	79 ± 51
	10	20 ± 5	4 ± 1

[a] Tissue concentrations were determined by the analysis of tissue samples from the 40 mg/kg dose groups via an ELISA-based assay.

Surprisingly, the tissue concentrations of the PNA conjugates did not correlate well with the observed activity. While conjugate **9** showed the best activity in adipose tissue, it was inactive in liver at a similar concentration. The minimally modified PNA **10** did not show activity in kidney at a μM tissue level similar to the octa(L-lysine) conjugate **9**. The fact that **10** was essentially inactive in all tissues examined can be explained by its unfavorable PK and reduced cellular uptake due to the lack of the peptide carrier. The high kidney concentration observed for PNA **10** was probably a consequence of increased filtration of unbound compound by the glomerulus and subsequent reabsorbtion by the kidney rather than its enhanced cellular uptake in this tissue. Similar phenomena with respect to antisense oligonucleotides have been reported.[13] These findings suggest that the peptide carrier plays an important role in determining the PK properties of the conjugates.

The tissue concentrations shown in Table 3 and the splicing activity shown in Figure 2 were utilized to determine PK/PD relationships. Table 4 summarizes the PK/PD results of the PNA conjugate **9** in comparison to the gapmer **7**, the value of which was determined in a previous study.[14] The observed potency difference for conjugate **9** in white adipose tissue compared to liver and kidney is likely due to the unique morphology of unilocular adipocytes, the major cell type of this tissue. A large fraction of up to 95−99% of the cell volume, based on the intracellular water content, is occupied by the lipid droplet, while cytoplasm and nucleus constitute only a small fraction of the total volume.[15]

Table 4. PK/PD Correlation in Liver and Adipose Tissue for the Octa(L-lysine) Conjugate **9** in Comparison to the 2′-*O*-MOE Gapmer **7**

compd	liver EC_{50} [μM]	adipose EC_{50} [μM]
9	> 100	70−80
7	14	0.7−1.4

Considering its hydrophilic, cationic nature, the PNA conjugate is expected to accumulate in the aqueous compartments and its effective concentration in the cytoplasm and nuclei of those cells should be 20−100-fold higher than the levels determined from the whole tissue. A similar concentration effect was also observed for the 2′-*O*-MOE gapmer **7**, which shows a 10−20-fold potency increase in adipose tissue compared to liver.

The EC_{50} results also imply that the 2′-*O*-MOE gapmer is approximately 100-fold more potent in vivo than the octa(L-lysine) PNA conjugate. While an intrinsic potency difference due to different mechanisms of action can be expected, it does not appear to be the major cause for the dramatically reduced in vivo potency of the PNA conjugate **9**, as potencies of RNase H acting and splicing antisense oligonucleotides are similar in cell culture (see results in Table 1). It is likely that reduced in vivo potency is a result of inefficient tissue and intracellular distribution of the PNA conjugate, leading to diminished localization at its site of action in the nucleus.

In Vivo Evaluation of an Octa(L-lysine) PNA Conjugate and a Uniform 2′-*O*-MOE Antisense Oligonucleotide Targeting the Murine Insulin Receptor. To test the generality of our findings, we evaluated compounds designed to alter splicing of mouse insulin receptor (IR) mRNA. Alternative splicing of insulin receptor RNA is reported to regulate insulin signaling (for a review, see Sesti et al., 2001).[16] The alternatively spliced form reflects a loss of exon 11, resulting in a loss of 12 amino acids in the α subunit. The isoforms produced by these two transcripts have been termed IR-A, corresponding to the transcript lacking exon 11, and IR-B, corresponding to the transcript including exon 11. Relative expression levels of the two isoforms vary among tissues, with liver and fat expressing mainly the IR-B isoform.[17] To determine if our findings from the PTEN PNA study would apply to another target sequence, we designed an

Table 5. Sequence and Dosing of the Peptide−PNA Conjugate **12** and Its Uniform 2′-*O*-MOE Control **13**

compd	sequence N to C-terminus (5′ to 3′)	dosing
12	$(Lys)_8$-ACCT$_K$[a]ACTGTCCTCGGCACCA-Lys	6.0, 1.5 μmol/kg; 3×/wk, 2 wks
13	ACCTACTGTCCTCGGCACCA[b]	6.0, 1.5 μmol/kg; 3×/wk, 2 wks

[a] T_K, (2-aminoethyl)lysine T. [b] Uniform 2′-*O*-MOE phosphorothioate (underlined).

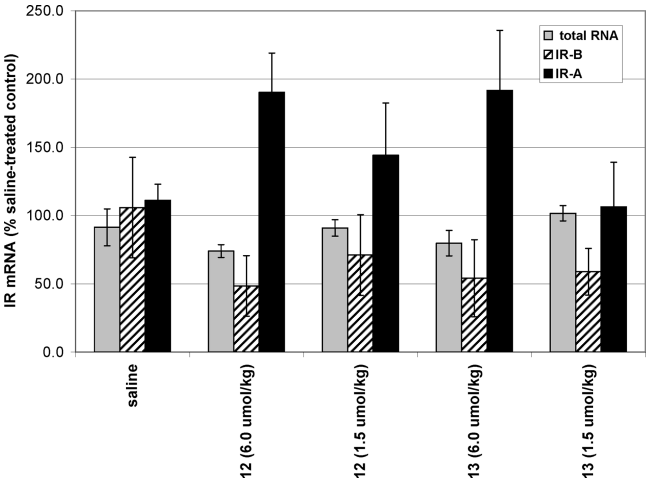

Figure 5. Antisense effects measured by quantitative RT-PCR analysis of IR RNA from adipose tissue.

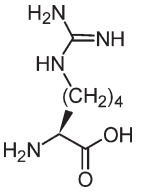

Figure 6. The amino acid homoarginine.

octa(L-lysine) PNA conjugate and a sequence matched uniform 2′-*O*-MOE antisense oligonucleotides (Table 5) and evaluated their ability to alter splicing of mouse IR primary transcript to favor production of the IR-A isoform in liver, kidney, and adipose tissue.

Animals were dosed ip (n = 4 per group) according to the indicated schedule and sacrificed 48 h after the last administration. Compounds **12** and **13** were administered at concentrations of 10.5, 6.0, and 1.5 μmol/kg and at a frequency of three times per week for two weeks (Table 5). The high dose of compound **12** displayed acute toxicity in mice, as determined by loss of body weight, and was terminated after the first administration. All other dose levels showed no adverse effects regarding weight gain, spleen and liver weight, as well as plasma chemistries.

mRNA from liver, kidney, and adipose tissue was analyzed by quantitative RT-PCR for the presence of different IR transcripts. Compounds **12** and **13** showed marginal activity in liver and kidney samples. The uniform 2′-*O*-MOE **13** showed a slight reduction of the IR-B transcript in liver at the 6.0 μmol/kg dose with a large increase of the IR-A transcript (see Supporting Information). The low dose of compound **13** as well as both doses of compound **12** caused an increase in IR-A but showed little corresponding decrease in IR-B transcript, which indicated low splicing activity of these compounds in liver tissue. In kidney, both doses of compounds **12** and **13** showed an increase in IR-A transcript without a concomitant down regulation of IR-B transcript (see Supporting Information).

However, alteration of splicing was again observed in adipose tissue for the PNA conjugate **12** (Figure 5). At 6.0 μmol/kg (39 mg/kg), the IR-B transcript was reduced by 50% and the IR-A transcript was upregulated by nearly 200% with respect to the saline-treated control group. An equivalent effect was observed for the uniform 2′-*O*-MOE administration at 6.0 μmol/kg (48 mg/kg). The activity for both the PNA conjugate **12** and the uniform 2′-*O*-MOE **13** is less dramatic at the lowest dose, which suggest that both compounds behave in a dose responsive fashion.

In Vivo Evaluation of PNA Conjugates Bearing Basic Amphipathic Peptides. In an attempt to improve further the biodistribution and cellular uptake of PNA conjugates, we extended our studies to structurally more complex peptides with an amphipathic-helical component. Previously, we reported on a series of basic amphipathic model peptides and identified a number of peptide motifs capable of efficient cellular delivery of antisense PNA in cell culture.[7] On this basis, we designed two PNA conjugates to be evaluated in vivo, one containing an enzymatically stabilized (all D-amino acids) lysine-rich peptide (**14**) and one bearing a peptide rich in arginines and homoarginines (hR, Figure 6) (**15**). These compounds in addition to their positive controls **7** and **9** were administered to healthy mice (Table 6).

Animals were dosed ip according to the indicated schedule (n = 4 per group) and sacrificed 48 h after administration of the last dose. The high dose group treated with conjugate **14** exhibited rapid weight loss after administration of the first dose, indicative of acute toxicity, which made it necessary to terminate this arm of the study prematurely. The animals had drastically reduced spleen sizes. Histopathological examination of the kidneys showed profound proximal tubule necrosis and proteinacous accumulation in Henle's loop and collecting tubules. An increased abundance of T-cells was found in the white pulp of the spleens. The liver morphology appeared normal. The study was completed for the low dose group of this conjugate. Histopathological examination of the kidneys of these animals, however, also showed nephrotoxicity with proximal tubule necrosis and regeneration, albeit less pronounced than with the single administration of the high dose. None of the other treatment groups of this study showed any significant changes in body weight, organ weight, or serum chemistry.

Neither of the PNA conjugates showed any significant activity in liver (data not shown). In kidney, conjugate **15** bearing the arginine-rich peptide was inactive (Figure 7a). However, the activity of the lysine-rich peptide conjugate **14** was comparable to the octa(L-lysine) conjugate **9**, even when administered at an approximately 4.5-fold lower dose. In adipose tissue, all PNA-conjugates displayed significant activity (Figure 7b). While the amphipathic peptide conjugate **14** showed activity at the low dose, conclusions about its potency relative to **9** were prohibited because the high dose results were compromised by its toxicity. Conjugate **15**, however, appears to be more potent than **9** as it altered splicing of PTEN mRNA to the same extent at a 2-fold lower

Table 6. Peptide Sequence and Dosing of the Amphipathic Peptide−PNA Conjugates **14** and **15** and Their Controls **7** and **9**

compd	sequence N to C-terminus (5′ to 3′)	dosing
9	$(Lys)_8$-T_K[a]CTCAGCACATCTACA-Lys	37 mg/kg, 3×/wk, 2 wks 25 mg/kg, 2×/d, 5 d
14	D-(KKLLKAALKLAKKG)-T_KCTCAGCACATCTACA-Lys	33 mg/kg, 3×/wk, 2 wks 8.25 mg/kg, 3×/wk, 2 wks
15	GhR[b]RAFhRRAhRhRhRFhRR-T_KCTCAGCACATCTACA-Lys	12.5 mg/kg, 2×/d, 5 d 2.5 mg/kg, 2×/d, 5 d
7	CTGCTAGCCTCTGGATTTGA	40 mg/kg, 3×/wk, 2 wks

[a] T_K, (2-aminoethyl)lysine T. [b] hR, homoarginine.

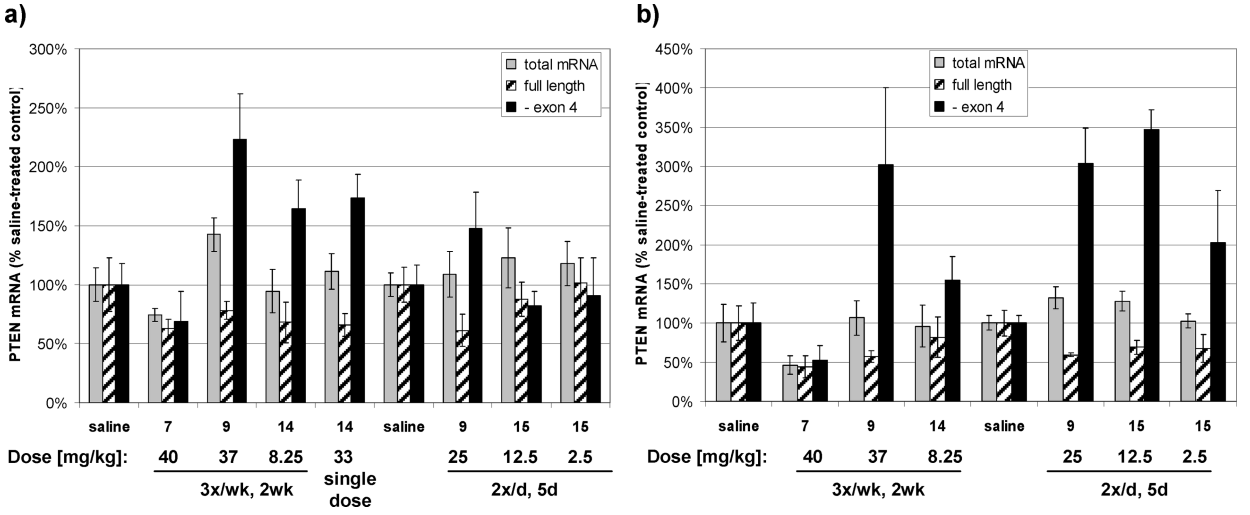

Figure 7. Antisense effects measured by quantitative RT-PCR analysis of PTEN mRNA in (a) kidney and (b) adipose tissue.

dose (Figure 7b). Even at a dose of 2.5 mg/kg, this compound displayed significant activity in adipose tissue.

Conclusion

The results from the studies described above demonstrated that PNA antisense oligomers conjugated to short cationic peptides are capable of eliciting dose-dependent and sequence-specific modulation of splicing in cell culture as well as in vivo. Conjugation of PNA to short basic peptides allowed for the accumulation of conjugate in liver, kidney, and adipose tissue. Nevertheless, cogent activity was only observed in adipose tissue.

The activity in adipose tissue compared to liver and kidney is likely due to the particular morphology of adipocytes, which contain large lipid depots occupying the majority of the cell volume. On the basis of the intracellular water-to-lipid ratio, the effective concentration of PNA in the cytoplasm and nucleus should be about 20−100-fold higher compared to the overall tissue levels determined bioanalytically. A similar increase in effective concentration and hence potency enhancement should occur in other cells, which accumulate large lipid deposits due to pathological changes. The amount of lipid accumulated as lipid droplets, for instance, is substantially elevated in hepatocytes of patients with fatty liver disease and in striated muscle in animal models of type 2 diabetes.[18,19]

Our studies established that the observed tissue distribution and antisense activity of the PNA conjugates were clearly dependent on the presence of a peptide carrier. Basic peptides of different lengths and sequences were capable of eliciting similar effects on gene expression. The generality of our findings was corroborated by an additional in vivo study in which an octa(L-Lysine) PNA conjugate showed compelling alteration of splicing of the murine insulin receptor mRNA in fat but less so in liver or kidney.

Interestingly, it appears that PNA conjugates accumulate in adipose tissues at high concentrations. However, results from our current as well as previous studies indicate that the PNA−peptide conjugates tested were approximately 2 orders of magnitude less potent than RNase H-based antisense oligonucleotides in adipose tissue. While an intrinsic potency difference due to different mechanisms of action might be expected, it appears unlikely as the major cause for this dramatic potency shift as evidenced by similar potency in cell culture.

While the mechanism by which permeation peptides traverse cellular membranes and gain entrance into the cytosol remains elusive, it is generally believed that endocytosis is an integral step in the permeation process for cationic peptides.[20−22] Upon endocytosis, a race ensues between the permeation peptides escape from the endosome and its degradation by endosomal proteases. Therefore, if the peptide portion of the conjugate is degraded prior to edosomal escape, the PNA portion of the conjugate will be trapped in this nonfunctional compartment. We believe that inefficient intracellular compartmentalization is responsible for diminished localization of the conjugate at its site of action in the nucleus. The PNA may be sequestered into a nonfunctional compartment because of peptide instability and degradation. Efforts to improve PNA potency by stabilizing the peptide portion of the drug resulted in toxicity, raising further concerns about this type of approach. These findings not only show the challenges of PNA−peptide conjugates for systemic applications but also underline the surprisingly efficient tissue delivery and intracellular trafficking of conventional phosphorothioate oligonucleotides. While achieving a significant hurdle by improving tissue distribution of PNA through the use of peptide conjugates,

it is clear that additional efforts are still required to transform PNA into a competitive clinical antisense therapeutic.

Experimental Section

Reagents and Solvents. The solvents used were purchased from Aldrich, Burdick & Jackson, or EMD in the highest grade available. Amino acids, the resins used for solid phase synthesis, HBTU, and HOBt were purchased from Novabiochem. PNA monomers (Boc-protected), HATU, and *N*-Boc-8-amino-3,6-dioxaoctanoic acid were obtained from Applied Biosystems. Cell culture reagents were obtained from Invitrogen. All other reagents were purchased from Sigma-Aldrich Corporation.

Synthesis, Purification, and Characterization of PNAs and PNA−Peptide Conjugates. PNAs and the PNA part of the peptide conjugates were assembled on MBHA polystyrene resin, preloaded with Boc-Lys(2-*Cl*-Z) (loading: 175 μmol/g) using a 433 A peptide synthesizer (Applied Biosystems) according to previously published procedures for PNA synthesis.[23,24] The synthesis of the peptide part of the conjugate was carried out manually and in parallel either with Fmoc- or Boc-chemistry using custom fabricated glass columns, equipped with a glass frit, a stop-cocked outlet, and an argon inlet. Deprotection and cleavage was generally carried out using a low/high TFMSA treatment, and the duration of the treatment was determined by the side chain protecting groups present.

The conjugates were purified by RP-HPLC using a Gilson HPLC system including a 306 piston pump system, a 811C dynamic mixer, a 155 UV/vis detector, and a 215 liquid handler together with the Unipoint software on Zorbax SB300 C_3 column (Agilent). Heptafluorobutyric acid 0.1% in H_2O (A) and CH_3CN (B) were used as the solvent system. The applied gradient was dependent on the length and sequence of the conjugate. Dual wavelength detection was carried out at 220 and 260 nm, and the column temperature was kept at 60 °C. Compounds were stored at −20 °C.

The purified PNA compounds were analyzed by mass spectrometry (ESI-MS) and the purity obtained by analytical HPLC utilizing the conditions described above. Purity of the ASO compounds was determined by analytical HPLC using a Waters XBridge C18 column (2.1 mm × 50 mm). Tributylammonium acetate (5 mM) in 20% CH_3CN/H_2O (solvent A) and tributylammonium acetate (5 mM) in 10% H_2O/CH_3CN (solvent B) were used as the solvent system. The purity of the compounds tested was ≥95% unless otherwise noted below.

Compound **1**: 87.8% purity; 20−70% B/8 min, ASO gradient conditions.

Compound **2**: 95.3% purity; 20−70% B/8 min, ASO gradient conditions.

Compound **3**: 99.9% purity; 0−35% B/30 min, PNA gradient conditions.

Compound **4**: 99.9% purity; 0−35% B/30 min, PNA gradient conditions.

Compound **5**: 99.9% purity; 0−35% B/30 min, PNA gradient conditions.

Compound **6**: 99.9% purity; 0−35% B/30 min, PNA gradient conditions.

Compound **7**: 94.8% purity; 20−70% B/8 min, ASO gradient conditions.

Compound **8**: 88.1% purity; 0−35% B/30 min, PNA gradient conditions.

Compound **9**: 99.9% purity; 0−60% B/30 min, PNA gradient conditions.

Compound **10**: 89.5% purity; 0−60% B/30 min, PNA gradient conditions.

Compound **11**: 99.9% purity; 0−60% B/30 min, PNA gradient conditions.

Compound **12**: 99.1% purity; 0−50% B/30 min, PNA gradient conditions.

Compound **13**: 87.9% purity; 20−70% B/8 min, ASO gradient conditions.

Compound **14**: 98.9% purity; 0−60% B/30 min, PNA gradient conditions.

Compound **15**: 99.5% purity; 0−50% B/30 min, PNA gradient conditions.

Cells. BCL_1 cells were obtained from the American Type Culture Collection and grown in normal growth medium (Dulbecco's Modified Eagle Medium, supplemented with 10% fetal bovine serum and antibiotics). Cells were incubated in a humidified chamber at 37 °C, containing 5% CO_2. PNA conjugates were added to cells at the indicated final concentrations. Where free uptake was used for compound delivery, cells were exposed to compound for 3 days. Where electroporation was used to deliver compounds within the cells, 2×10^6 cells were electroporated at the noted compound concentrations in a 0.2 cm cuvette utilizing an Electro Cell Manipulator 600 (Biotechnologies and Experimental Research, Inc.) with the determined optimal settings (200 V 1000 μF, 13 Ω). Post electroporation, cells were suspended into 10 mL of complete culture media, and 2 mL were plated into a single well of a 6-well plate. Incubation continued for 24 h (RNA) or 72 h (protein). All experiments were done in triplicate.

RT-PCR. Tissues were homogenized in 4 M guanidine isothiocyanate, 25 mM EDTA, 50 mM Tris-HCl pH 6 immediately following sacrifice. RNA was extracted using RNeasy columns (Qiagen) according to manufacturer's protocol. RNA was eluted from the columns with water. RNA samples were analyzed by fluorescence-based quantitative RT-PCR using an Applied Biosystems 7700 sequence detector. Levels of target RNAs as well as those of cyclophilin A, a housekeeping gene, were determined. Target RNA levels were normalized to cyclophilin levels for each RNA sample. For the sequences of the primers and probes used to quantify each transcript, see Supporting Information Table S2.

Western Blots. Samples were homogenized in RIPA buffer (PBS containing 1% NP-40, 0.5% sodium deoxycholate, 0.1% SDS) containing Complete protease inhibitors (Roche), and protein concentrations were determined by Lowry assay (BioRad). Protein samples were separated on a 10% PAGE gel (Invitrogen) and subsequently transferred to a PVDF membrane (Invitrogen). Membranes were incubated at room temperature in blocking buffer consisting of 5% nonfat dry milk in TBS-T for 1 h. Rabbit polyclonal antiPTEN antibodies were obtained from Cell Signaling and Upstate Biotechnology and were used at 1:1000 dilution. Rabbit polyclonal antibody to mouse CD40 was obtained from Calbiochem and used at 1:1000 dilution. HRP conjugated antirabbit secondary antibodies were obtained from Jackson Immunoresearch and were used at 1:2500 dilution. Protein bands were visualized using ECL-plus reagent (Amersham).

Animal Treatment. Male Balb/c mice, aged 6−8 weeks, were obtained from Charles River Laboratories. Compounds were suspended in phosphate buffered saline, filter sterilized, and administered by intraperitoneal (ip) injection according to the indicated dosing schedules in a volume corresponding to 10 μL/g based on animal weight. Animals were maintained at a constant temperature of 23 °C and were allowed standard lab diet and water ad libitum, and animal weights were monitored throughout the live phase of the study. Immediately prior to sacrifice, mice were anesthetized with isoflurane and terminal bleeds were performed by cardiac puncture. Serum was isolated from whole blood and analyzed for transaminase levels. Serum ALT elevations were considered absent if less than 2× normal, mild if 2×−4× normal, moderate for 4×−10× normal, and severe if greater than 10× normal. Mice were sacrificed by cervical dislocation. In conjunction with necropsy, liver and spleen weights were determined.

ELISA-Based Assay for PNA Quantitation in Tissue Samples. Tissue samples were minced and placed into fast-prep tubes. Extraction buffer (8 mM Tris, 8 mM EDTA, 40 mM NaCl, 0.4% SDS, pH 8.1) was added to yield a tissue concentration of

100 mg/mL, and the samples were homogenized in a fast-prep shaker and kept frozen at −80 °C until before further use. An aliquot of each sample was further diluted with extraction buffer to a final tissue concentration of 0.2 mg/mL. Hybridization to the cutting probe with a sequence complementary to the analyte (TGTAGATGTGCTGAGA), which was 5′-modified with digoxigenin spaced via an hexylaminolinker and 3′-modified with biotin spaced via triethylene glycol linker, was carried out in Axygen 96 well PCR plates as follows: To 60 μL of each analyte solution per well was added 60 μL of hybridization buffer (24 mM Tris, 600 mM NaCl, 26.4 mM MgCl, 1.2% SDS, pH 9.1) containing 200 nM of the cutting probe and 200 nM of a nonsequence-related oligonucleotide to prevent nonspecific binding. On the same plate, a concentration ladder was prepared from standard solutions for each analyte with final concentrations of 100, 40, 10, 4, 1, and 0.1 nM as described above. Each sample was prepared in quadruplicate. The plates were sealed with aluminum foil adhesive and shaken carefully before they were heated to 75 °C for 5 min and incubated overnight at 37 °C. After the plates were cooled to rt, they were centrifuged and the aluminum cover was carefully removed. Using a multichannel pipettor, 100 μL of each well were transferred to its respective well on a clear NeutrAvidin-coated 96-well plate (Pierce). The plates were covered and incubated at rt for 45 min. After removing the solutions from the wells, the plates were three times washed on a plate washing station (MAP-C, Titertek) with stringency buffer containing 20 mM Tris, 1 M $NaClO_4$, 0.1% Tween 20, pH 7.2. Subsequently, 100 μL of a solution containing 5.4% glycerol, 32.3 mM NaAc, 1.1 mM ZnAc, 650 mM NaCl, and 326 units/mL of nuclease S1 was added to each well and the plates were covered and shaken carefully before the solutions were allowed to incubate at rt for 2 h. Again, the plates were washed three times with stringency buffer as described above, before 100 μL of a solution containing 0.5 μL of Anti-Digoxigenin-AP (150 U/200 μL, Roche) in 10% Super Block blocking buffer (Pierce) was added to each well. After incubation for 30 min, the plates were washed four times with buffer containing 50 mM Tris, 0.9% NaCl, and 0.1% Tween 20, pH 7.2, as described above. Then 100 μL of AttoPhos AP fluorescent substrate system (Promega) was added to each well, and the plates were sealed with Axygen film, shaken carefully, and allowed to incubate for 20 min in the dark before an additional 50 μL of saturated Na_2HPO_4 solution was added to each well. The plates were read on a Cytofluor instrument using the following parameters: excitation: 450/50, emission: 580/50, gain: 45. The raw data was sorted and filtered based on the critical ratio (*R* value) with a cutoff of 0.679. Tissue concentrations of the analyte samples were calculated from the background corrected data points based on regression analysis of the calibration curves.

Acknowledgment. We thank Gene Hung for the histopathological examination of the tissues. Professor Corey acknowledges the National Institutes of Health (NIH 60642 and NIH 73042) and the Robert A. Welch Foundation (I-1244) for financial support.

Supporting Information Available: Tabular analytical data (HPLC and ESI-MS) for compounds; representative example of HPLC and ESI-MS analysis data for compound **9**; PTEN Western blot and RT-PCR data and primer probe sequence table. This material is available free of charge via the Internet at http://pubs.acs.org.

References

(1) Nielsen, P. E.; Egholm, M.; Berg, R. H.; Buchardt, O. Sequence-selective recognition of DNA by strand displacement with a thymine-substituted polyamide. *Science* **1991**, *254*, 1497–1500.
(2) Egholm, M.; Buchardt, O.; Christensen, L.; Behrens, C.; Freier, S. M.; et al. PNA hybridizes to complementary oligonucleotides obeying the Watson−Crick hydrogen-bonding rules. *Nature* (*London*) **1993**, *365*, 566–568.
(3) Demidov, V. V.; Potaman, V. N.; Frank-Kamenetskii, M. D.; Egholm, M.; Buchard, O.; et al. Stability of peptide nucleic acids in human serum and cellular extracts. *Biochem. Pharmacol.* **1994**, *48*, 1310–1313.
(4) Mardirossian, G.; Lei, K.; Rusckowski, M.; Chang, F.; Qu, T.; et al. In vivo hybridization of technetium-99m-labeled peptide nucleic acid (PNA). *J. Nucl. Med.* **1997**, *38*, 907–913.
(5) McMahon, B. M.; Mays, D.; Lipsky, J.; Stewart, J. A.; Fauq, A.; et al. Pharmacokinetics and tissue distribution of a peptide nucleic acid after intravenous administration. *Antisense Nucleic Acid Drug Dev.* **2002**, *12*, 65–70.
(6) Albertshofer, K.; Siwkowski, A. M.; Wancewicz, E. V.; Esau, C. C.; Watanabe, T.; et al. Structure−activity relationship study on a simple cationic peptide motif for cellular delivery of antisense peptide nucleic acid. *J. Med. Chem.* **2005**, *48*, 6741–6749.
(7) Maier, M. A.; Esau, C. C.; Siwkowski, A. M.; Wancewicz, E. V.; Albertshofer, K.; et al. Evaluation of basic amphipathic peptides for cellular delivery of antisense peptide nucleic acids. *J. Med. Chem.* **2006**, *49*, 2534–2542.
(8) Knudsen, H.; Nielsen, P. E. Antisense properties of duplex- and triplex-forming PNAs. *Nucleic Acids Res.* **1996**, *24*, 494–500.
(9) Wu, H.; Lima, W. F.; Zhang, H.; Fan, A.; Sun, H.; et al. Determination of the role of the human RNase H1 in the pharmacology of DNA-like antisense drugs. *J. Biol. Chem.* **2004**, *279*, 17181–17189.
(10) Siwkowski, A. M.; Malik, L.; Esau, C. C.; Maier, M. A.; Wancewicz, E. V.; et al. Identification and functional validation of PNAs that inhibit murine CD40 expression by redirection of splicing. *Nucleic Acids Res.* **2004**, *32*, 2695–2706.
(11) Sazani, P.; Kang, S.-H.; Maier, M. A.; Wei, C.; Dillman, J.; et al. Nuclear antisense effects of neutral, anionic and cationic oligonucleotide analogs. *Nucleic Acids Res.* **2001**, *29*, 3965–3974.
(12) Sazani, P.; Gemignani, F.; Kang, S.-H.; Maier, M. A.; Manoharan, M.; et al. Systemically delivered antisense oligomers upregulate gene expression in mouse tissues. *Nat. Biotechnol.* **2002**, *20*, 1228–1233.
(13) Crooke, S. T. Antisense Drug Technology: Principles, *Strategies, and Applications*, 2nd ed.; CRC Press: Boca Raton, 2007; pp 183−215.
(14) Butler, M.; McKay, R. A.; Popoff, I. J.; Gaarde, W. A.; Witchell, D.; et al. Specific inhibition of PTEN expression reverses hyperglycemia in diabetic mice. *Diabetes* **2002**, *51*, 1028–1034.
(15) DiGirolamo, M.; Owens, J. L. Water content of rat adipose tissue and isolated adipocytes in relation to cell size. *Am. J. Physiol.* **1976**, *231*, 1568–1572.
(16) Sesti, G.; Federici, M.; Lauro, D.; Sbraccia, P.; Lauro, R. Molecular mechanism of insulin resistance in type 2 diabetes mellitus: role of the insulin receptor variant forms. *Diabetes Metab. Res. Rev.* **2001**, *17*, 363–373.
(17) Benecke, H.; Flier, J. S.; Moller, D. E. Alternatively spliced variants of the insulin receptor protein. Expression in normal and diabetic human tissues. *J. Clin. Invest.* **1992**, *89*, 2066–2070.
(18) Wolf, A. M.; Busch, B.; Kuhlmann, H. W.; Beisiegel, U. Histological changes in the liver of morbidly obese patients: correlation with metabolic parameters. *Obes. Surg.* **2005**, *15*, 228–237.
(19) Fraenkel, M.; Weiss, R.; Leizerman, I.; Anaby, D.; Golomb, E.; et al. Scanning electron microscopic analysis of intramyocellular lipid droplets in an animal model of type 2 diabetes. *Obesity* **2008**, *16*, 695–699.
(20) Wadia, J. S.; Stan, R. V.; Dowdy, S. F. Transducible TAT-HA fusogenic peptide enhances escape of TAT-fusion proteins after lipid raft macropinocytosis. *Nat. Med.* **2004**, *10*, 310–315.
(21) Richard, J. P.; Melikov, K.; Brooks, H.; Prevot, P.; Lebleu, B.; et al. Cellular uptake of unconjugated TAT peptide involves clathrin-dependent endocytosis and heparan sulfate receptors. *J. Biol. Chem.* **2005**, *280*, 15300–15306.
(22) Gerbal-Chaloin, S.; Gondeau, C.; Aldrian-Herrada, G.; Heitz, F.; Gauthier-Rouviere, C.; et al. First step of the cell-penetrating peptide mechanism involves Rac1 GTPase-dependent actin-network remodelling. *Biol. Cell* **2007**, *99*, 223–238.
(23) Christensen, L.; Fitzpatrick, R.; Gildea, B.; Petersen, K. H.; Hansen, H. F.; et al. Solid-phase synthesis of peptide nucleic acids. *J. Pept. Sci.* **1995**, *1*, 185–183.
(24) Koch, T.; Hansen, H. F.; Andersen, P.; Larsen, T.; Batz, H. G.; et al. Improvements in automated PNA synthesis using Boc/Z monomers. *J. Pept. Res.* **1997**, *49*, 80–88.